Published in final edited form as:
Development. 2008 June ; 135(12): 2093–2103. doi:10.1242/dev.015990.

Gli3 coordinates three-dimensional patterning and growth of the tectum and cerebellum by integrating Shh and Fgf8 signaling

Sandra Blaess, **Daniel Stephen**, and **Alexandra L. Joyner***
Developmental Biology Program, Memorial Sloan-Kettering Cancer Center 1275 York Avenue, Box 511, New York, NY 10021, Tel: 1 212-639-3962, Fax: 1 212-717-3738

Summary

The coordination of anterior-posterior (AP) and dorsal-ventral (DV) patterning of the mesencephalon (mes) and rhombomere1 (r1) is instrumental for the development of three distinct brain structures: the tectum and cerebellum dorsally and the tegmentum ventrally. Patterning of the mes/r1 is primarily mediated by signaling molecules secreted from two organizers: Sonic Hedgehog (Shh) from the floor plate (DV) and Fgf8 from the isthmus (AP). Gli3, a zinc finger transcription factor in the Shh signaling pathway, has been implicated in regulating *Fgf8* expression and therefore is a potential candidate for coordinating the action of the two organizers. By inactivating *Gli3* at successive embryonic time points in vivo, we uncovered the extent and the underlying mechanism of Gli3 function in the mes/r1. We demonstrate that before E9.0, *Gli3* is required for establishing a distinct posterior tectum, isthmus and cerebellum, but does not play a role in the development of the tegmentum. Between E9.0 and E11.0 *Gli3* continues to be required for isthmus and cerebellar development, but primarily for defining the cerebellar foliation pattern. We show that *Gli3* regulates patterning of the isthmus and cerebellar anlage by confining *Fgf8* expression to the isthmus and attenuates growth of dorsal r1 (before E11.0) and the dorsal mes and isthmus (beyond E11.0) through regulation of cell proliferation and viability. In conclusion, our results show that *Gli3* is essential for the coordinated three-dimensional patterning and growth of the dorsal mes/r1.

Introduction

A fundamental question in developmental neuroscience is how the simple mammalian neural tube is transformed into the complex and intricate structures that constitute the adult brain. Patterning of tissues in three dimensions requires precise coordination of a number of basic developmental processes including cell proliferation, specification and migration. An ideal system to study patterning events is the brain region consisting of the mesencephalon (mes) and rhombomere1 (r1). The mes and r1 are the primordia for the tectum (superior colliculus (SC) and inferior colliculus (IC)) and cerebellum dorsally, respectively, and the tegmentum ventrally. Organizing centers that govern mes/r1 growth and patterning along the dorsal-ventral (DV) and anterior-posterior (AP) axes have been identified. AP patterning of the mes/r1 is mediated by Fibroblast growth factor 8 (Fgf8), which is secreted by the isthmic organizer located at the mes/r1 boundary (Wurst and Bally-Cuif, 2001; Zervas et al., 2005). Sonic Hedgehog (Shh), expressed in the notochord and the ventral midline (floor plate) of the neural tube, controls specification of ventral cell types in the tegmentum and formation of normal dorsal structures, as well as cell proliferation and survival (Agarwala et al., 2001; Bayly et al., 2007; Blaess et al., 2006; Corrales et al., 2006; Fedtsova and Turner, 2001; Ishibashi and McMahon, 2002). It remains to be addressed how these two signaling centers are integrated to control growth and patterning in three dimensions.

*Correspondence: E-mail: joynera@mskcc.org.

The zinc finger transcription factor Gli3 influences multiple signaling pathways in the mes/r1. Gli3 is an essential downstream component of the Shh signaling pathway, and an increase in Gli3 repressor (Gli3R) levels is the primary cause of the dorsal mes/r1 defects in Shh signaling mutants (Blaess et al., 2006). Furthermore, Gli3 plays a role in regulating the *Fgf8* expression domain at the mes/r1 boundary (Aoto et al., 2002). Therefore, Gli3 could play a key role in coordinating three-dimensional patterning of the mes/r1 by affecting these two signaling pathways.

Only one mutation in mouse that is thought to represent a *Gli3* null allele has been characterized. The lethal *Gli3 extratoe (Xt)* mutation causes multiple defects, including a background dependent occurrence of exencephaly (Hui and Joyner, 1993; Maynard et al., 2002). In non-excencephalic embryos, however, tectum- and cerebellum-like structures develop, but are morphologically highly abnormal (Aoto et al., 2002; Blaess et al., 2006). The analysis of $Gli3^{Xt/Xt}$ mutants has so far given little insight into Gli3 function in the mes/r1 as it remains unclear whether the defects result from changes in the expression of key DV patterning genes, abnormal growth and/or changes in Fgf8 signaling in the isthmic organizer (Aoto et al., 2002).

Gli3 transcription and protein activity is regulated at many levels by Shh signaling. In the absence of Shh activity Gli3 is processed into an N-terminal repressor form that suppresses Shh target genes (Hu et al., 2006; Wang et al., 2000). Shh signaling attenuates the level of Gli3R, and full-length Gli3 can act as a weak activator (Gli3A) when the concentration of Shh is high (Bai et al., 2004; Dai et al., 1999; Wang et al., 2007). Gli3, however, is also transcriptionally down regulated in cells receiving high levels of Shh. Consequently, *Gli3* expression, which is initially found throughout the neural plate, is restricted to the intermediate and dorsal neural tube after E8.5 (Bai et al., 2002; Blaess et al., 2006; Hui et al., 1994; Marigo et al., 1996).

Activation of Shh target genes is primarily mediated by Gli1 and Gli2 (Fuccillo et al., 2006; Jacob and Briscoe, 2003). Gli2 requires Shh signaling to act as an activator (Gli2A) while Gli1 is a transcriptional target of Gli2/3A and is itself a constitutive activator (Fuccillo et al., 2006; Jacob and Briscoe, 2003). We recently showed that Gli2A-mediated Shh signaling is the key regulator of the initial specification of ventral neurons in the embryonic mes/r1 before E11 and granule cell precursor proliferation in the postnatal cerebellum (Blaess et al., 2006; Corrales et al., 2006; Corrales et al., 2004). It is unclear, however, whether Gli3A also is required for the development of these two regions.

Analysis of the severely abnormal $Gli3^{Xt/Xt}$ null mutants can only provide insight into the first critical early developmental function of Gli3. To study the underlying mechanisms of Gli3 function we combined analysis of null and time specific conditional mutants by generating a *Gli3* conditional allele and inactivating *Gli3* in the mes/r1 at either E9.0 or E11.5. We demonstrate that *Gli3* is required to pattern dorsal mes/r1 into distinct structures before E9.0, continues to regulate the growth of the tectum and the cerebellum as well as cerebellar foliation between E9.0 and E11.0, and plays a role beyond E11.0 in regulating growth of the isthmus, SC and IC. We further show that the role of Gli3 in isthmic and cerebellar development, but not tectal patterning, is largely mediated through repression of *Fgf8* expression in r1.

Material and Methods

Generation of Gli3 conditional mutants

A 5.8 kb *PstI-MfeI* genomic fragment of *Gli3* containing intron 8 was inserted into a targeting vector upstream of a *neo* cassette flanked with *Frt* sites, with one loxP site 3′ to the *neo* cassette and a *TK* cassette. Another loxP site containing an *EcoRV* site was inserted into a *Nhe*I site

within intron 9 in a 4.8 kb *MfeI-KpnI* genomic fragment of *Gli3*. This fragment was inserted 3′ to the loxP site in the *neo-TK* vector.

Three targeted W4 (Auerbach et al., 2000) ES cell clones were identified (Matise et al., 2000) by Southern blot analysis using SphI and a 1 kb external probe 3′ of the *SphI* site or using *KpnI* and an internal probe containing *neo*. ES cell chimeras were generated through injection of C57BL/6 blastocysts (Skirball Transgenic Facility)(Papaioannou and Johnson, 2000). Chimeras were bred to C57BL/6 mice and heterozygous $Gli3^{flox\text{-}neo/+}$ offspring to SV129 *ACTB-Flpe* mice (Rodriguez et al., 2000) to produce $Gli3^{flox/+}$ heterozygotes lacking *neo*. $Gli3^{rec/+}$ mice carrying a loxP mediated deletion were intercrossed or crossed with $Gli3^{Xt/+}$ mice (Hui and Joyner, 1993). Both $Gli3^{rec/rec}$ and $Gli3^{rec/Xt}$ E18.5 embryos displayed the same brain and limb phenotypes described in $Gli3^{Xt/Xt}$ embryos (Fig. S1D–F) (Hui and Joyner, 1993). Other phenotypes observed in $Gli3^{Xt/Xt}$ embryos, such as lethality at birth and exencephaly in some mutants were also observed (data not shown). The $Gli3^{flox}$ allele was genotyped using the following primers: S1, 5′-CTGGATGAACCAAGCTTTCCATC-3′; AS3, 5′-CTGCTCAGTGCTCTGGGCTCC- 3′. For detecting the recombined allele, primers were S1 (see above) and AS2 5′-CAGTAGTAGCCTGGTTACAG-3′.

Other alleles were genotyped as described: *Cre*, Smo^{flox}, Smo^{rec} (Blaess et al., 2006), *Fgf8* null (Chi et al., 2003) and $Gli3^{Xt}$ null (Maynard et al., 2002). $Gli3^{Xt/+}$ mice were maintained on a C57/BL6 background, all other mouse lines were maintained on an outbred Swiss Webster background. Noon of the day a vaginal plug was observed was designated as E0.5; the day of birth was designated as P0.

Histology, immunohistochemistry and RNA in situ hybridization

Embryos/brains were fixed in 4% paraformaldehyde (PFA) at 4°C, processed for paraffin- or cryosectioning and sectioned at 7–12 μm. Antibody staining, BrdU labeling and RNA in situ hybridization were performed using standard methods. Primary antibodies : rabbit-TH (Chemicon, 1:500); rabbit-Ki67 (NovoCastra, 1:500); mouse-BrdU (BD-Bioscience, 1:100); rabbit anti-PH3 (1:500; Cell Signaling Technology); rabbit-Caspase3 (Cell Signaling Technology, 1:200); mouse-Calbindin (Sigma, 1:1000); rabbit-Calbindin (Swant, 1:5000); rabbit-Pax2 (Zymed, 1:500); rabbit-neurogranin (Chemicon, 1:500), mouse-Nkx6.1 ((Pedersen et al., 2006) Developmental Studies Hybridoma Bank, 1:100). Apoptosis was quantified with immunostaining for cleaved Caspase-3. Proliferation and/or cell cycle exit was quantified using Phosphohistone-3 (PH-3) immunostaining or BrdU pulse labeling (1 hr or 24 hrs) followed by BrdU, BrdU/Ki67 immunostaining. Coronal sections of wild-type and conditional mutants (≥ 3 embryos for each genotype and stage) were used. In situ hybridization and/or immunostaining for region specific markers (En1: mes/r1 at E9.5, Otx2: mes, Pax7: dorsal mes/r1, Pax6: diencephalon) was performed on adjacent sections. Cells were counted in the ventral and dorsal mes and r1 (≥ 3 sections) at E9.5 and E10.5 and either normalized for ventricle length (cleaved Caspase-3, PH-3) or total cell number (BrdU). At E12.5, cells in the dorsal mes (≥ 3 sections) and in r1 and ventral mes (1–3 sections) were counted and normalized for ventricle length (PH-3) or cell number (BrdU+, Ki67+/BrdU+). Cell counts were performed using ImageJ. Detailed protocols are available at http://www.mskcc.org/mskcc/html/77387.cfm.

Results

Distinct temporal contributions of *Gli3* to growth and patterning of the midbrain and cerebellum

To study Gli3 function, we generated mice carrying a conditional *Gli3* mutant allele, $Gli3^{flox}$, in which two loxP sites flank exon 8 (Fig. S1 in Supplementary Material). Deletion

of exon 8 and splicing from exon 7 to 9 results in a frameshift mutation upstream of the DNA binding domain (*Gli3*^{rec}). Since we previously showed that a short period of gene function can be sufficient to rescue the most severe defects observed in null mutants (Blaess et al., 2006; Sgaier et al., 2007), *En1-Cre* was used to remove *Gli3* specifically in the mes/r1 by E9.0, about 36 hrs after the onset of *Gli3* expression (Hui et al., 1994; Kimmel et al., 2000; Li et al., 2002) (Fig. S2). To assess whether Gli3 is required for mes/r1 development after midgestation, *Nestin-Cre* was used to remove *Gli3* in the entire neural tube around E11.5 (Blaess et al., 2006; Graus-Porta et al., 2001; Tronche et al., 1999) (Fig. S2). Indeed, inactivation of *Gli3* by E9 (*Gli3*$^{flox/Xt}$*;En1-Cre* mice, referred to as *En1-Gli3* cko) or E11.5 (*Gli3*$^{flox/Xt}$*;Nestin-Cre* mice, referred to as *Nes-Gli3* cko) resulted in rescue of the early postnatal lethality of *Gli3* null mutants and the conditional knock-out mice survived for several months.

The *Gli3* conditional mutants were first compared to *Gli3* null mutants at E18.5, since the latter die at birth. *Gli3* null mutants (*Gli3*$^{Xt/Xt}$, *Gli3*$^{Xt/rec}$ or *Gli3*$^{rec/rec}$) showed a consistent but variable phenotype in the midbrain and cerebellum at E18.5 (Fig. S3A–J), but the variability was independent of the allele (*rec* or *Xt*). Therefore all three genotypes were used to represent the *Gli3* null (*Gli3*$^{-/-}$) mutant phenotype. At the gross morphological level the phenotype of E18.5 *Gli3*$^{-/-}$ mutants included (1) a poorly foliated cerebellum which was not clearly separated from the isthmus; (2) an expanded isthmus-like region with ectopic cell clusters; (3) an overgrown tectum; (4) loss of the distinct morphology that normally defines the isthmus, IC and SC (8/11) (Figs 1A,B,E,F; S3A–J). In contrast, the tegmentum of *Gli3*$^{-/-}$ mutants was morphologically unaffected and the size of the ventral nuclei comprised of tyrosine hydroxylase (TH) positive dopaminergic neurons or Isl1 positive motoneurons appeared similar to wild-type (WT) mice (Fig. 1I,J; and data not shown).

Similar to *Gli3*$^{-/-}$ mutants, E18.5 *En1-Gli3* cko mutants had a normal tegmentum, and a misshapen and enlarged tectum and isthmus (Figs 1C,G,K; S3K,L). In contrast to *Gli3*$^{-/-}$ mutants, however, the isthmus, IC and SC each appeared as morphologically distinct structures in the majority of *En1-Gli3* cko mutants (9/16). Furthermore, the cerebellum was well developed, appeared to have a normal cytoarchitecture and had begun to foliate, although the foliation pattern was abnormal (Figs 1C,G; 3O–Q; S3K,L and data not shown). When *Gli3* function was left intact until E11.5 (*Nes-Gli3* cko mutants) all the morphological defects in the cerebellum, isthmus and tectum were rescued at E18.5 (Fig. 1A,D,E,H), but the size of the isthmus and the entire tectum was significantly increased (Figs 1A,D,E,H,L; S3M,N).

In summary, histological analysis indicates that *Gli3* is required for the dorsal mes/r1 primordium to form distinct brain structures before E9.0 and to establish the cerebellar foliation pattern and the normal size and shape of the isthmus and tectum between E9 and E11. Furtehrmore, *Gli3* regulates growth of the tectum and isthmus beyond E11.5.

Gli3 is required to regulate mes and r1 growth

To assess when the mes/r1 phenotypes arise in *Gli3* mutants, we analyzed E10.5 (*Gli3*$^{-/-}$ and *En1-Gli3* cko) and E12.5 (all mutants) embryos. We observed severe morphological defects in the mes/r1 of *Gli3*$^{-/-}$ and *En1-Gli3* cko mutant embryos, which in general were more pronounced in *Gli3*$^{-/-}$ mutants (Figs 1M–O and data not shown): (1) the mesencephalic ventricle was expanded, (2) dorsal posterior mes, isthmus and r1 were morphologically not distinct from each other and the isthmic flexure was less prominent, (3) the thickness of the ventricular zone of the posterior dorsal mes, isthmus and r1 region was increased.

The increased growth of the mes/r1 in *Gli3* mutant embryos could either be caused by a decrease in cell death or an increase in proliferation. A previous whole mount analysis suggested that cell death is decreased in the mes/r1 at E8.5 and in the mes dorsal midline at E9.5 in *Gli3*$^{-/-}$ mutants (Aoto et al., 2002). To investigate whether decreased cell death could underlie the

expansion of dorsal mes/r1 in *Gli3* mutant embryos we analyzed the number of cleaved Caspase-3 positive cells in the mes/r1 of E9.5 and E10.5 *En1-Gli3* cko mutants. There was a trend toward decreased cell death in *En1-Gli3* cko mutants compared to WT, but only in the E10.5 dorsal mes/r1 (Fig. S4D,E). Since these results indicate that cell death is not dramatically reduced in the absence of *Gli3*, reduced cell death is however unlikely to be the sole cause of mes/r1 overgrowth in the mutants.

To address whether increased proliferation contributes to the increase in mes/r1 size we analyzed ventral and dorsal mes/r1 of WT and cko mutant embryos for BrdU incorporation (1 hour pulse, S-phase of the cell cycle) or for expression of Phosphohistone-3 (G2/M-phase of the cell cycle). Quantitative assessment of proliferating cells indicated a slight increase in proliferation in the dorsal mes/r1 of *En1-Gli3* cko mutants at E9.5 and E10.5 and in the dorsal mes of E12.5 *Nes-Gli3* cko mutants compared to WT (Fig. S4A–C). Importantly, in the ventral mes/r1, proliferation appeared to be similar in cko mutants and WT consistent with the lack of a ventral phenotype at E18.5. Since an increased proliferation rate could either be caused by shortening of cell cycle length or a delay in differentiation, we analyzed the cell cycle exit rate in E12.5 WT and *Nes-Gli3* cko mutants (Chenn and Walsh, 2002). We quantified the percentage of differentiating cells ($BrdU^+Ki67^-$ cells/$BrdU^+$ cells) 24 hrs after BrdU administration and did not observe an obvious changes between WT and mutant in ventral or dorsal mes or r1 (Fig. S4F). Thus, the increase in proliferation is not due to a decreased ability of cells to leave the cell cycle. In summary, these data demonstrate that *Gli3* is an important regulator of the growth of dorsal r1 (up to E11.0) and mes (beyond E11.0), by modulating both, cell proliferation (attenuation) and cell death (augmentation).

Gli3 is required for proper establishment of the inferior colliculus before E9.0

To investigate whether the abnormal tectal morphology in *Gli3* mutants is due to the observed mes overgrowth or to a direct requirement for *Gli3* in tectal patterning, we analyzed the expression of SC and IC markers at E18.5. We used *En1* as a marker for the IC, since *En1* is normally expressed strongly throughout the IC and at lower levels in the posterior SC (Fig. 2A). *Otx2* was used as an SC marker, since its expression in the superficial layers of the SC is clearly distinguishable from the *Otx2* expression in the IC ventricular zone (Fig. 2E). In $Gli3^{-/-}$ mutants, *En1* expression was very weak and was confined to the most posterior tectum (3/3), even in mutants in which the tectum appeared to be organized into a SC and IC at a morphological level (2/3) (Fig. 2B). In *En1-Gli3* cko mutants, *En1* expression was stronger and broader than in $Gli3^{-/-}$ mutants but was restricted to a more posterior tectal region than in WT brain (3/3) (Fig. 2C). These data indicate that the IC was not properly specified in the mutants. This was also evident by *Otx2* expression, which was not restricted to the ventricular layer of the posterior tectum in $Gli3^{-/-}$ and *En1-Gli3* cko mutants. In addition, the thickness of the *Otx2* positive layer was increased in the SC of $Gli3^{-/-}$ and *En1-Gli3* cko mutants, consistent with the tectal overgrowth in these mutants. As expected, given the normal tectal morphology of E18.5 *Nes-Gli3* cko mutants, the *En1* and *Otx2* expression domains were comparable to WT (Fig. 2A,E,D,H).

Despite the abnormal *En1* and *Otx2* expression in the posterior tectum, this region was not transformed into SC in the mutants, since the AP extent of the *Otx2* expression domain in the superficial layers of the SC was comparable to WT in $Gli3^{-/-}$ and *En1-Gli3* cko mutants (Fig. 2F,G). Furthermore, Neurogranin, which is expressed in differentiated cells in the lateral IC at E18.5 and the entire IC at P16 (Fig. 2I,L) was found to be expressed in the lateral tectum of E18.5 $Gli3^{-/-}$ mutants. The Neurogranin expression domain, however, was severely reduced and shifted anteriorly (3/3) (Fig. 2J). In P16 *En1-Gli3* cko mutants Neurogranin immunostaining revealed a more elongated IC domain than in WT (Fig. 2L,M). In contrast, the shape of the IC was comparable to WT in P16 *Nes-Gli3* cko mutants, even though the size

of the IC was increased (Fig. 2L,N). These data indicate that *Gli3* is required for proper establishment of the IC before E9.0, regulates normal IC morphology between E9.0-E11.0 and growth beyond E11.0. In contrast, *Gli3* is not required for establishing the SC although it plays a prolonged role in controlling normal SC growth.

Gli3 regulates proper establishment of the isthmus and cerebellum before E9.0 and cerebellar foliation between E9.0 and E11.0

To study the cellular phenotype of the isthmus-cerebellum-like region in $Gli3^{-/-}$ mutants we analyzed markers for cerebellar and isthmic cell types. In the E18.5/P0 WT cerebellum, Purkinje cells are organized in a layer underlying Math1 positive granule cell precursors in the external granule cell layer (Fig. 3A,C,F,I). At this stage, all Purkinje cells express the receptor-related orphan receptor-alpha (RORα), while a large subset expresses Calbindin and Inositol 1,4,5-trisphosphate receptor type 1 (IP3R1) (Fig. 3F,I and data not shown). Pax2 is expressed throughout the isthmus and deeper cerebellum where it marks (among other cell types) a subset of interneuron precursors (Fig. 3L) (Maricich and Herrup, 1999).

In $Gli3^{-/-}$ mutants, the cerebellar external granule cell layer did not extend into the anterior area of the medial isthmus-cerebellum-like region, suggesting that the anterior region might be transformed into isthmus (Figs 1B; 3B,D). This anterior area, however, did not contain Pax2 positive cells, but instead had clusters of RORα and IP3R1 positive Purkinje cells, indicating that this region had some characteristics of the cerebellum rather than the isthmus (Fig. 3G,J,M and data not shown). The organization of the posterior isthmus-cerebellum-like region had some similarities to WT cerebellum, with a relatively normal distribution of Pax2 positive cells and RORα and IP3R1 positive Purkinje cells underlying a Math1 positive external granule cell layer (Fig. 3B,D,G,J,M and data not shown). The Purkinje cell layer, however, was thicker than normal and did not consistently extend into the most posterior area. In addition, Purkinje cell axons that form bundles in WT were highly disorganized in $Gli3^{-/-}$ mutants (Fig. 3F,G and data not shown). This disorganization of Purkinje cells was equally severe in more lateral regions of the cerebellum (data not shown). These results indicate that the anterior isthmic-cerebellar region is not properly specified in $Gli3^{-/-}$ mutants and the posterior isthmus-cerebellum area is not organized into a normal cerebellar cytoarchitecture.

In P0 *En1-Gli3* cko mutants, the defects in cerebellar cytoarchitecture were partially rescued, based on marker analysis (Fig. 3E,H,K,N and data not shown). Purkinje cell axons projected aberrantly into the posterior isthmus and some Purkinje cells formed clusters in the anterior isthmic region (Fig. 3H,K), suggesting that the isthmus-cerebellum boundary was not properly established in *En1-Gli3* cko mutants. Furthermore, at E18.5 and all the postnatal stages analyzed (P2, P5, P8, P16, P30), the cerebellar foliation pattern was clearly abnormal and variable between mutants (Figs 3O-Q; S3K,L and data not shown). Interestingly, these defects in foliation were not associated with major changes in anterior-posterior gene expression domains, since expression of *Otx2* (posterior region) and *Runx1* (central region) in the external granule cell layer were comparable to WT (data not shown). Consistent with the histological analysis, the cytoarchitecture, morphology and foliation pattern of E18.5 and postnatal *Nes-Gli3* cko cerebella were similar to WT (Fig. 1A,D and data not shown). In conclusion, *Gli3* is required primarily before E9.0 for the proper specification of the isthmus and cerebellum, including the formation of normal cerebellar cytoarchitecture and between E9.0 and E11.0 for establishing the stereotypic cerebellar foliation pattern.

Gli3R is not involved in attenuating GliA-mediated signaling in the dorsal mes/r1

Since Shh signaling induces ventral structures in the neural tube, one possible reason for the abnormal patterning of the IC, isthmus and cerebellum in $Gli3^{-/-}$ and *En1-Gli3* cko mutants is a Shh-induced ventralization of dorsal structures. To address this, we investigated whether

the expression of ventrally (*Gli1, Nkx2.2* and *Nkx6.1*) and dorsally (*Pax7, Gbx2, EphrinA5*) restricted genes is altered in the mes/r1 of *Gli3* mutants. Surprisingly, no dorsal expansion of *Gli1, Nkx2.2* or Nkx6.1 was observed in *Gli3*$^{-/-}$ and *En1-Gli3* cko mutants (Fig. 4D–I and data not shown). Furthermore, in both, *Gli3*$^{-/-}$ and *En1-Gli3* cko mutants, *Pax7* encompassed a similar dorsal domain as in WT embryos, indicating further that the dorsal mes/r1 was not ventralized in *Gli3* mutants (Fig. 4A–C). In addition, expression of *Gbx2* in dorsal r1 and *EphrinA5* in dorsal-posterior mes was maintained in *Gli3*$^{-/-}$ and *En1-Gli3* cko mutant embryos (data not shown). In summary, these results show that *Gli3* does not play a major role in establishing DV spatial molecular patterning in the mes/r1.

The unaltered DV gene expression domains in *Gli3* mutants indicate that there is no ectopic GliA-mediated Shh signaling activity in the dorsal mes/r1 in the absence of *Gli3*. To definitively demonstrate that GliA-mediated Shh signaling does not contribute to the patterning and growth defects in *Gli3* mutants we generated double cko mutants for *Smo* and *Gli3* (*En1-Gli3;Smo* cko), since removal of *Smo* results in absence of GliA activity. Indeed, we found that E12.5 and P0 *En1-Gli3;Smo* cko mutant embryos had a tectal and isthmus phenotype very similar to *En1-Gli3* cko mutants (Fig. 4K–M; compare Fig. 4J with Fig. 1C; data not shown). The morphology and overgrowth of r1 in *En1-Gli3;Smo* cko mutants was also similar to *En1-Gli3* cko mutants at E12.5. At P0, the overall size of the cerebellum and thickness of the external granule cell layer, however, was reduced (Fig. 4J and data not shown) resembling the *En1-Smo* cko phenotype that results from severely decreased granule cell precursor proliferation after E16.5 (Blaess et al., 2006; Corrales et al., 2006). This indicates that the overgrowth in the *En1-Gli3;Smo* cko cerebellar anlage is initially caused by loss of Gli3R (before E16.5), while after E16.5 the loss of Gli1/2A–mediated Shh signaling downstream of Smo results in reduced cerebellar growth due to decreased granule cell precursor proliferation. In summary these data demonstrate that the initial phenotypes in the dorsal mes/r1 of *Gli3* mutants result from a loss of Gli3R activity rather than ectopic GliA mediated Shh signaling.

Gli3 is not required for roof plate induction in the mes/r1

Since defects in the roof plate contribute to the telencephalic phenotype in *Gli3*$^{-/-}$ mutants (Grove et al., 1998; Theil et al., 2002), we assessed whether alterations of signaling from the mes/r1 roof plate cause the dorsal mes/r1 phenotypes in *Gli3* mutants. Expression of two secreted factors involved in the organizing function of the roof plate, *Wnt1* and *Gdf7*, however, was maintained in the roof plate of *Gli3*$^{-/-}$ and *En1-Gli3* cko embryos at E9.5 and E10.5 (Fig. 5A–F and data not shown). In addition, *Msx1*, which is a downstream target of BMP signaling (Alder et al., 1999; Bei and Maas, 1998) was present in the roof plate in *Gli3*$^{-/-}$ and *En1-Gli3* cko mutants (Fig. 5G,H, and data not shown). Finally, expression of *Axin2*, a target of Wnt signaling (Jho et al., 2002), was not grossly altered in E10.5 *Gli3*$^{-/-}$ or *En1-Gli3* cko mutant embryos (Fig. 5I,J and data not shown). In summary, *Gli3* does not appear to play a major role in establishing or maintaining the mes roof plate.

Gli3R is required to downregulate *Fgf* in dorsal r1

Since changes in DV patterning or roof plate signaling do not seem to account for the dorsal mes/r1 phenotype in *Gli3* mutants, we next examined whether alterations in the Fgf8 signaling pathway, which is a primary regulator of AP patterning, could contribute to the dorsal mes/r1 defects in *Gli3* mutants. Based on wholemount analysis, it was reported that *Fgf8* expression is expanded in E9.5 and E10.5 *Gli3*$^{-/-}$ mutants, while the *Fgf8* domain is reduced when Shh signaling is decreased and Gli3R is increased (Aoto et al., 2002; Blaess et al., 2006). We first analyzed *Fgf8* expression in spatial and temporal detail on sagittal sections of *Gli3* mutant embryos. Indeed, we observed ectopic *Fgf8* expression, but only in medial r1 in both E9.5 and E10.5 *Gli3*$^{-/-}$ (Fig. 6G–I and data not shown) and *En1-Gli3* cko mutants (data not shown). By E12.5, shortly before the normal termination of *Fgf8* expression, ectopic *Fgf8* expression was

restricted to the posterior most part of medial r1 in *Gli3*$^{-/-}$ (data not shown) and *En1-Gli3* cko mutants (Fig. 6J,K). Interestingly, this region corresponds to the rhombic lip in the WT and normally expresses *Wnt1* and *Math1* (Fig. 6A,B,D,E and data not shown). Furthermore, *Fgf17*, which also plays a role in AP patterning of the mes/r1 and is expressed in a broader domain than *Fgf8* in the WT (Xu et al., 2000), and *Sprouty1* (*Spry1)*, a direct target of Fgf8 signaling (Liu et al., 2003) were expanded posteriorly in both *Gli3* mutants, but were not altered in the mes (Fig. 6M–Q,S–W). To address whether Gli3R rather than Shh signaliung is required for *Fgf8* suppression in r1 we analyzed E12.5 *En1-Gli3;Smo* cko mutants and found that similar to *En1-Gli3* cko mutants, *Fgf8, Fgf17* and *Spry1* were expressed ectopically in dorsal-posterior r1 (data not shown).

Consistent with the normal tectal and cerebellar morphology in *Nes-Gli3* cko mutants, no changes in *Fgf8, Fgf17* or *Spry1* expression were observed in these mutants at E12.5 (Fig. 6F,L,R,X). In addition, in all *Gli3* mutants, the expression domains of *Wnt1* and *Otx2* in the mes appeared normal (anterior to *Fgf8* expression) and *Gbx2* expression in r1 was maintained (Fig. 6A–F and data not shown). These results indicate that changes in gene expression are specific to the Fgf pathway and that the boundary between the mes and r1 is intact in *Gli3* mutants. Thus, Gli3R is required to inhibit *Fgf8* and *Fgf17* expression beyond E9.0, but only in dorsal-medial r1.

Gli3 mediates isthmic and cerebellar patterning through regulation of Fgf8 expression

To test whether the expansion of *Fgf* expression in r1 is responsible for any of the dorsal defects in *Gli3* mutants, we removed one copy of *Fgf8* in *Gli3*$^{-/-}$ mutants. Histological analysis of *Gli3*$^{-/-}$*; Fgf8*$^{+/-}$ mutants (n=4) at E18.5 or P0 showed a striking partial rescue of the defects seen in the isthmus-cerebellum-like region, but not the tectum of *Gli3*$^{-/-}$ mutants (Fig. 7 and Fig. S5). Unlike any of the *Gli3*−/− littermates, the cerebellum of all *Gli3*−/−; *Fgf8*+/− mutants had begun to foliate at P0 and the external granule cell layer extended along the AP length of the medial cerebellum (Fig. 7A,E, see Fig. S5A–H for a direct comparison of littermates). In addition, the isthmus appeared to have formed, based on morphology and expression of Pax2 (Fig. 7A,H Fig. S5A–H). Marker analysis further revealed a more normal organization of Purkinje cells, although cell clusters remained in and near the isthmus region, showing that a separation of isthmus and cerebellum was not fully established (Fig. 7F,G; Fig. S5I,J).

While the isthmus-cerebellar phenotype was partially rescued in the *Gli3*$^{-/-}$*; Fgf8*$^{+/-}$ mutants compared to *Gli3*$^{-/-}$ single mutants, the tectal phenotype was similar to *Gli3*$^{-/-}$ single mutants. The tectum was enlarged, the IC was not clearly distinguishable and the range of morphological abnormalities was comparable to *Gli3*$^{-/-}$ mutants (Figs 7A; 1B; S3A,C,E,G,I; S5). Furthermore, *En1*, *Otx2* and Neurogranin were abnormally expressed in the posterior tectum similar to in *Gli3*$^{-/-}$ mutants (Figs 7B–D; 2A,B,E,F). These findings provide genetic evidence that a major role of Gli3R in regulating organization of cerebellar and isthmic cytoarchitecture is to localize *Fgf8* expression to dorsal-medial r1.

Discussion

Distinct temporal functions of Gli3 in midbrain and cerebellum development

By studying the sequential cellular and genetic changes underlying *Gli3* function in mes/r1 development we demonstrate that Gli3R is a critical regulator of growth and patterning of the dorsal mes/r1, whereas neither Gli3R nor Gli3A are required for development of the ventral mes/r1 (summarized in Fig. 8A). We show that dorsally, Gli3 has a prolonged role in attenuating growth of r1 (before E11.0) and the mes and isthmus (beyond E11.0) through reducing cell proliferation and promoting cell death. Importantly, analysis of *Gli3;Smo* double mutants demonstrates that normally it is Gli3R that attenuates growth in the mes/r1 and that

factors other than Shh must stimulate mes/r1 proliferation. We further show that Gli3R has additional functions in patterning of the dorsal mes/r1. Before E9.0, Gli3R is required to establish a normal IC and a distinct isthmus and anterior cerebellum as well as a normal cytoarchitecture. Between E9.0 and E11.0 Gli3R prevents Purkinje cells and their axons from entering the isthmus and is involved in setting up a normal foliation pattern. Finally, we demonstrate that the loss of the distinct separation between isthmus and cerebellum in *Gli3* null mutants as well as the abnormal cytoarchitecture in this region, is caused by ectopic expression of *Fgf8* in r1.

Gli3R is required to restrict *Fgf8* expression to the isthmus

We and others showed previously that *Fgf8* expression in the isthmic organizer is reduced when Gli3R is upregulated (*Shh/Smo* mutants) and increased when *Gli3* is absent ($Gli3^{-/-}$ mutants) (Aoto et al., 2002; Blaess et al., 2006). We built on these findings by showing that complete absence of *Gli3* as well as inactivation of *Gli3* at E9.0 (*En1-Gli3* cko mutants) results in an expanded expression domain of not only *Fgf8*, but also *Fgf17* and the Fgf8 downstream target *Spry1*. Furthermore, the expansion occurs only in the dorsal-medial region of r1 and interestingly this region includes the rhombic lip region. Moreover, the ectopic Fgf expression in r1 in the absence of *Gli3* is not diminished when Shh signaling is abolished (*En1-Gli3;Smo* cko mutants). Thus, Gli3R and not Shh activator signaling is required to restrict *Fgf8/Fgf17* expression to the isthmus. These results raise the question whether Gli3 might regulate *Fgf8* expression directly. Sequence analysis of the known Fgf8 regulatory elements (Beermann et al., 2006), however, did not reveal any canonical Gli binding sites (Vokes et al., 2007) in these conserved regions (S.B and Jaden Hastings, unpublished).

Fgf8 expression in the WT mes/r1 initially encompasses the isthmus and most of dorsal r1 at E8.5 and then becomes restricted to the isthmus by E10.5 (Crossley and Martin, 1995). While there is evidence that the transcription factors *Otx2* and *Grg4* are normally involved in repression of Fgf8 in the mes, it was unclear how Fgf8 becomes downregulated in dorsal r1 (Ye et al 2001). Our study of *Gli3* mutants indicates a role for Gli3R in the initial down regulation of *Fgf8* in r1, as well as a continued requirement until after E9.0 in maintaining the dorsal restriction of *Fgf8* to the isthmus. Alternatively, Gli3 might be required to maintain dorsal-medial r1 identity and the expansion of *Fgf8* expression is a secondary consequence of a mixed r1/isthmus identity. Interestingly, a similar interaction between Shh, Gli3 and Fgf8 exists in the developing telencephalon (Gutin et al., 2006; Kuschel et al., 2003; Ohkubo et al., 2002), suggesting that the interplay between these two signaling pathways provides a more general mechanism in patterning of three-dimensional brain structures.

Regulation of cerebellum and isthmus development by Gli3R is dependent on restricting *Fgf8* to the isthmus

Based on Fgf8 loss- and gain-of-function studies the observed ectopic expression of *Fgf8* in dorsal r1 of *Gli3* mutants could affect both tectum and cerebellum development (Zervas et al., 2005). To test this possibility we analyzed $Gli3^{-/-}$ mutants in which one copy of *Fgf8* was removed. Strikingly, we found that while the isthmic-cerebellar region phenotype is partially rescued in $Gli3^{-/-};Fgf8^{+/-}$ mutants, the defects in tectal growth and IC patterning were largely not attenuated. The lack of influence of Fgf8 on mes development is likely because a high enough level of Fgf8 signaling is not attained in the mes, consistent with the observation that *Spry1* is not obviously upregulated in the mes of *Gli3* mutants.

Interestingly, even though *Fgf8* expression is expanded in both $Gli3^{-/-}$ and *En1-Gli3* cko mutants at E10.5, the cerebellar defects are much more severe in $Gli3^{-/-}$ mutants. In $Gli3^{-/-}$ mutants, the cerebellar cytoarchitecture is severely altered and foliation is not initiated by P0. In contrast, inactivation of *Gli3* after E9.0 results in only mild cytoarchitectural defects in the

cerebellum and a normal onset of foliation, but abnormal foliation pattern. Preliminary analysis of *En1-Gli3* cko mutants in which one copy of *Fgf8* was removed found that the foliation pattern is still abnormal (S.B., unpublished). One possibility is that the foliation defects in *En1-Gli3* cko mutants are independent of ectopic Fgf8 and directly caused by the loss of *Gli3*.

Attenuation of mes growth by Gli3R

One striking phenotype in the *Gli3* null and cko mutants is the extensive overgrowth of tectal tissue. It has previously been shown that ectopic activation of the Shh pathway by misexpression of either Shh or GliA results in a pronounced overgrowth of the spinal cord, mes/r1 and postnatal cerebellum in chick and mouse (Cayuso et al., 2006; Corrales et al., 2006; Dahmane and Ruiz-i-Altaba, 1999; Rowitch et al., 1999). The increased size of the tectum that we documented in *Gli3* and *Gli3/Smo* mutants, however, demonstrates that removing Gli3R, without an associated ectopic activation of Gli activator function, can cause increased proliferation and overgrowth. Furthermore, Gli3R is normally required beyond E11.5 to attenuate growth of the dorsal mes.

Our present results taken together with previous studies (Blaess et al., 2006; Britto et al., 2002; Ishibashi and McMahon, 2002; Corrales et al., 2006) suggest several mechanisms by which Glis regulate tissue growth. At high levels of signaling, Shh, can simply increase proliferation by upregulating GliA (primarily Gli2) such as in cerebellar granule cell precursors (Corrales et al., 2006) or also by down regulating Gli3R such as in the ventral midbrain (Blaess et al., 2006). At low levels of Shh signaling, such as in the dorsal mes, GliA is not induced, and Shh increases overall growth only by down regulating Gli3R levels which leads to increased proliferation and cell survival (summarized in Fig. 8B). The latter reveals that other signaling pathways must stimulate proliferation of dorsal mes progenitors and a certain level of Gli3R is required only to attenuate growth.

A possible candidate to regulate proliferation in the dorsal mes is Wnt1 since it can induce overgrowth of the posterior mes (Panhuysen et al., 2004) and recent studies provided evidence that Gli3R inhibits canonical Wnt signaling in several different tissues and cell types (Alvarez-Medina et al., 2008; Ulloa et al., 2007). However, our analysis of *Axin2* expression (a readout for canonical Wnt signaling) in the mes of *Gli3* mutants provided no evidence that *Gli3* is required in the dorsal mes to antagonize Wnt signaling. Furthermore, our preliminary analysis of $Gli3^{-/-}$;$Wnt1^{sw/sw}$ double mutants revealed that the size of the SC is comparable to $Gli3^{-/-}$ mutants, although the IC (and medial cerebellum) are lost in both $Wnt1^{sw/sw}$ and $Gli3^{-/-}$;$Wnt1^{sw/sw}$ mutants (S.B., unpublished). It is possible, however, that additional members of the Wnt family stimulate dorsal mes growth and that their action is normally attenuated by Gli3R.

In summary, we have found that the precise regulation of Gli3R levels is critical to establish the intricate structures of the mature tectum and cerebellum. Our data provide insight into how Gli3R coordinates the function of two distinct organizer molecules in the mes/r1 by either modulating their expression or downstream signaling. It will be interesting to investigate whether Gli3R plays similar complex roles in other tissues that undergo organizer dependent three-dimensional patterning and growth.

Supplementary Material

Refer to Web version on PubMed Central for supplementary material.

Acknowledgements

We thank Drs F. Costantini and K. Millen for providing RNA in situ probes and the Developmental Studies Hybridoma Bank for the Nkx6.1 antibody. We are grateful to Frada Berenstehyn for excellent technical help, to Jaden Hastings for help with sequence analysis and to Anamaria Sudarov, Charles Levine, Emilie Legue and Roy Sillitoe for critical reading of the manuscript. This work was funded by grant R01 CA128158 from NICHD. S.B. was supported by a DFG postdoctoral fellowship.

References

Agarwala S, Sanders TA, Ragsdale CW. Sonic hedgehog control of size and shape in midbrain pattern formation. Science 2001;291:2147–50. [PubMed: 11251119]

Alder J, Lee KJ, Jessell TM, Hatten ME. Generation of cerebellar granule neurons in vivo by transplantation of BMP-treated neural progenitor cells. Nat Neurosci 1999;2:535–40. [PubMed: 10448218]

Alvarez-Medina R, Cayuso J, Okubo T, Takada S, Marti E. Wnt canonical pathway restricts graded Shh/Gli patterning activity through the regulation of Gli3 expression. Development 2008;135:237–47. [PubMed: 18057099]

Aoto K, Nishimura T, Eto K, Motoyama J. Mouse GLI3 regulates Fgf8 expression and apoptosis in the developing neural tube, face, and limb bud. Dev Biol 2002;251:320–32. [PubMed: 12435361]

Bai CB, Auerbach W, Lee JS, Stephen D, Joyner AL. Gli2, but not Gli1, is required for initial Shh signaling and ectopic activation of the Shh pathway. Development 2002;129:4753–61. [PubMed: 12361967]

Bai CB, Stephen D, Joyner AL. All mouse ventral spinal cord patterning by hedgehog is Gli dependent and involves an activator function of Gli3. Dev Cell 2004;6:103–15. [PubMed: 14723851]

Bayly RD, Ngo M, Aglyamova GV, Agarwala S. Regulation of ventral midbrain patterning by Hedgehog signaling. Development 2007;134:2115–24. [PubMed: 17507412]

Beermann F, Kaloulis K, Hofmann D, Murisier F, Bucher P, Trumpp A. Identification of evolutionarily conserved regulatory elements in the mouse Fgf8 locus. Genesis 2006;44:1–6. [PubMed: 16397882]

Bei M, Maas R. FGFs and BMP4 induce both Msx1-independent and Msx1-dependent signaling pathways in early tooth development. Development 1998;125:4325–33. [PubMed: 9753686]

Blaess S, Corrales JD, Joyner AL. Sonic hedgehog regulates Gli activator and repressor functions with spatial and temporal precision in the mid/hindbrain region. Development 2006;133:1799–809. [PubMed: 16571630]

Britto J, Tannahill D, Keynes R. A critical role for sonic hedgehog signaling in the early expansion of the developing brain. Nat Neurosci 2002;5:103–10. [PubMed: 11788837]

Cayuso J, Ulloa F, Cox B, Briscoe J, Marti E. The Sonic hedgehog pathway independently controls the patterning, proliferation and survival of neuroepithelial cells by regulating Gli activity. Development 2006;133:517–28. [PubMed: 16410413]

Chenn A, Walsh CA. Regulation of cerebral cortical size by control of cell cycle exit in neural precursors. Science 2002;297:365–9. [PubMed: 12130776]

Chi CL, Martinez S, Wurst W, Martin GR. The isthmic organizer signal FGF8 is required for cell survival in the prospective midbrain and cerebellum. Development 2003;130:2633–44. [PubMed: 12736208]

Corrales JD, Blaess S, Mahoney EM, Joyner AL. The level of sonic hedgehog signaling regulates the complexity of cerebellar foliation. Development 2006;133:1811–21. [PubMed: 16571625]

Corrales JD, Rocco GL, Blaess S, Guo Q, Joyner AL. Spatial pattern of sonic hedgehog signaling through Gli genes during cerebellum development. Development 2004;131:5581–90. [PubMed: 15496441]

Dahmane N, Ruiz-i-Altaba A. Sonic hedgehog regulates the growth and patterning of the cerebellum. Development 1999;126:3089–100. [PubMed: 10375501]

Dai P, Akimaru H, Tanaka Y, Maekawa T, Nakafuku M, Ishii S. Sonic Hedgehog-induced activation of the Gli1 promoter is mediated by GLI3. J Biol Chem 1999;274:8143–52. [PubMed: 10075717]

Fedtsova N, Turner EE. Signals from the ventral midline and isthmus regulate the development of Brn3.0-expressing neurons in the midbrain. Mech Dev 2001;105:129–44. [PubMed: 11429288]

Fuccillo M, Joyner AL, Fishell G. Morphogen to mitogen: the multiple roles of hedgehog signalling in vertebrate neural development. Nat Rev Neurosci 2006;7:772–83. [PubMed: 16988653]

Graus-Porta D, Blaess S, Senften M, Littlewood-Evans A, Damsky C, Huang Z, Orban P, Klein R, Schittny JC, Muller U. Beta1-class integrins regulate the development of laminae and folia in the cerebral and cerebellar cortex. Neuron 2001;31:367–79. [PubMed: 11516395]

Grove EA, Tole S, Limon J, Yip L, Ragsdale CW. The hem of the embryonic cerebral cortex is defined by the expression of multiple Wnt genes and is compromised in Gli3-deficient mice. Development 1998;125:2315–25. [PubMed: 9584130]

Gutin G, Fernandes M, Palazzolo L, Paek H, Yu K, Ornitz DM, McConnell SK, Hebert JM. FGF signalling generates ventral telencephalic cells independently of SHH. Development 2006;133:2937–46. [PubMed: 16818446]

Hu MC, Mo R, Bhella S, Wilson CW, Chuang PT, Hui CC, Rosenblum ND. GLI3-dependent transcriptional repression of Gli1, Gli2 and kidney patterning genes disrupts renal morphogenesis. Development 2006;133:569–78. [PubMed: 16396903]

Hui CC, Joyner AL. A mouse model of greig cephalopolysyndactyly syndrome: the extra-toesJ mutation contains an intragenic deletion of the Gli3 gene. Nat Genet 1993;3:241–6. [PubMed: 8387379]

Hui CC, Slusarski D, Platt KA, Holmgren R, Joyner AL. Expression of three mouse homologs of the Drosophila segment polarity gene cubitus interruptus, Gli, Gli-2, and Gli-3, in ectoderm- and mesoderm-derived tissues suggests multiple roles during postimplantation development. Dev Biol 1994;162:402–13. [PubMed: 8150204]

Ishibashi M, McMahon AP. A sonic hedgehog-dependent signaling relay regulates growth of diencephalic and mesencephalic primordia in the early mouse embryo. Development 2002;129:4807–19. [PubMed: 12361972]

Jacob J, Briscoe J. Gli proteins and the control of spinal-cord patterning. EMBO Rep 2003;4:761–5. [PubMed: 12897799]

Jho EH, Zhang T, Domon C, Joo CK, Freund JN, Costantini F. Wnt/beta-catenin/Tcf signaling induces the transcription of Axin2, a negative regulator of the signaling pathway. Mol Cell Biol 2002;22:1172–83. [PubMed: 11809808]

Kimmel RA, Turnbull DH, Blanquet V, Wurst W, Loomis CA, Joyner AL. Two lineage boundaries coordinate vertebrate apical ectodermal ridge formation. Genes Dev 2000;14:1377–89. [PubMed: 10837030]

Kuschel S, Ruther U, Theil T. A disrupted balance between Bmp/Wnt and Fgf signaling underlies the ventralization of the Gli3 mutant telencephalon. Dev Biol 2003;260:484–95. [PubMed: 12921747]

Li JY, Lao Z, Joyner AL. Changing requirements for Gbx2 in development of the cerebellum and maintenance of the mid/hindbrain organizer. Neuron 2002;36:31–43. [PubMed: 12367504]

Liu A, Li JY, Bromleigh C, Lao Z, Niswander LA, Joyner AL. FGF17b and FGF18 have different midbrain regulatory properties from FGF8b or activated FGF receptors. Development 2003;130:6175–85. [PubMed: 14602678]

Maricich SM, Herrup K. Pax-2 expression defines a subset of GABAergic interneurons and their precursors in the developing murine cerebellum. J Neurobiol 1999;41:281–94. [PubMed: 10512984]

Marigo V, Johnson RL, Vortkamp A, Tabin CJ. Sonic hedgehog differentially regulates expression of GLI and GLI3 during limb development. Dev Biol 1996;180:273–83. [PubMed: 8948590]

Maynard TM, Jain MD, Balmer CW, LaMantia AS. High-resolution mapping of the Gli3 mutation extra-toes reveals a 51.5-kb deletion. Mamm Genome 2002;13:58–61. [PubMed: 11773971]

Ohkubo Y, Chiang C, Rubenstein JL. Coordinate regulation and synergistic actions of BMP4, SHH and FGF8 in the rostral prosencephalon regulate morphogenesis of the telencephalic and optic vesicles. Neuroscience 2002;111:1–17. [PubMed: 11955708]

Panhuysen M, Vogt Weisenhorn DM, Blanquet V, Brodski C, Heinzmann U, Beisker W, Wurst W. Effects of Wnt1 signaling on proliferation in the developing mid-/hindbrain region. Mol Cell Neurosci 2004;26:101–11. [PubMed: 15121182]

Papaioannou, V.; Johnson, R. Production of chimeras by blastocyst and morula injection of targeted ES-cells. In: Joyner, AL., editor. Gene Targeting: A practical approach. Oxford: Oxford University Press; 2000. p. 133-175.

Pedersen IL, Klinck R, Hecksher-Sorensen J, Zahn S, Madsen OD, Serup P, Jorgensen MC. Generation and characterization of monoclonal antibodies against the transcription factor Nkx6.1. J Histochem Cytochem 2006;54:567–74. [PubMed: 16401696]

Rowitch DH, B SJ, Lee SM, Flax JD, Snyder EY, McMahon AP. Sonic hedgehog regulates proliferation and inhibits differentiation of CNS precursor cells. J Neurosci 1999;19:8954–65. [PubMed: 10516314]

Theil T, Aydin S, Koch S, Grotewold L, Ruther U. Wnt and Bmp signalling cooperatively regulate graded Emx2 expression in the dorsal telencephalon. Development 2002;129:3045–54. [PubMed: 12070081]

Tronche F, Kellendonk C, Kretz O, Gass P, Anlag K, Orban PC, Bock R, Klein R, Schutz G. Disruption of the glucocorticoid receptor gene in the nervous system results in reduced anxiety. Nat Genet 1999;23:99–103. [PubMed: 10471508]

Ulloa F, Itasaki N, Briscoe J. Inhibitory Gli3 Activity Negatively Regulates Wnt/beta-Catenin Signaling. Curr Biol. 2007

Vokes SA, Ji H, McCuine S, Tenzen T, Giles S, Zhong S, Longabaugh WJ, Davidson EH, Wong WH, McMahon AP. Genomic characterization of Gli-activator targets in sonic hedgehog-mediated neural patterning. Development 2007;134:1977–89. [PubMed: 17442700]

Wang B, Fallon JF, Beachy PA. Hedgehog-regulated processing of Gli3 produces an anterior/posterior repressor gradient in the developing vertebrate limb. Cell 2000;100:423–34. [PubMed: 10693759]

Wang C, Ruther U, Wang B. The Shh-independent activator function of the full-length Gli3 protein and its role in vertebrate limb digit patterning. Dev Biol 2007;305:460–9. [PubMed: 17400206]

Wurst W, Bally-Cuif L. Neural plate patterning: upstream and downstream of the isthmic organizer. Nat Rev Neurosci 2001;2:99–108. [PubMed: 11253000]

Xu J, Liu Z, Ornitz DM. Temporal and spatial gradients of Fgf8 and Fgf17 regulate proliferation and differentiation of midline cerebellar structures. Development 2000;127:1833–43. [PubMed: 10751172]

Zervas M, Blaess S, Joyner AL. Classical embryological studies and modern genetic analysis of midbrain and cerebellum development. Curr Top Dev Biol 2005;69:101–38. [PubMed: 16243598]

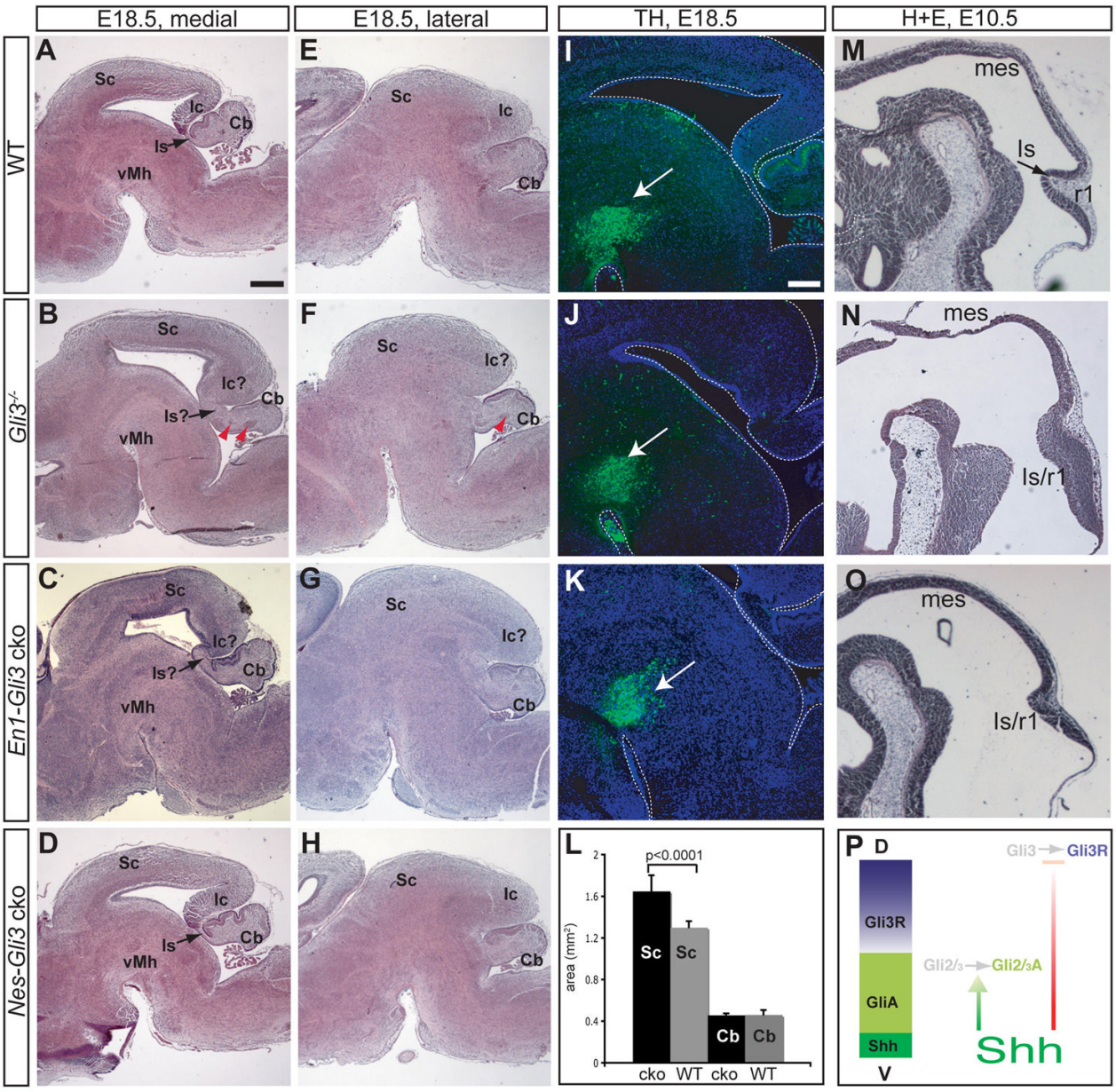

Fig. 1. Distinct temporal roles of *Gli3* in regulating midbrain and cerebellum development

(A–H) Hematoxylin and Eosin (H+E) staining of midline (A–D) and lateral (E–H) E18.5 sagittal brain sections. (B,F) In *Gli3*$^{-/-}$ mutants, the dorsal midbrain is enlarged and the distinct morphology of the inferior (Ic) and superior colliculus (Sc) is lost. Similarly, the isthmus (Is) and cerebellum (Cb) are not clearly separated and contain cell clusters (red arrowheads). The Cb is not foliated. The morphology of the ventral mid/hindbrain (vMh) appears normal. (C,G) In *En1-Gli3* cko mutants, the Sc, Ic, Is and Cb (arrow) are enlarged, and tectum, Is and Cb are morphological distinct from one another. The Cb foliation pattern is abnormal. (D,H) In *Nes-Gli3* cko mutants, the Sc, Ic, Is and Cb are morphologically distinct, but the Sc, Ic and Is are increased in size. (I–K) Immunohistochemistry for tyrosine hydroxylase (TH) shows no change in dopaminergic neurons (green, arrows) in the mutants. DAPI staining is in blue. (L) Quantitative assessment of Cb and Sc size in WT and *Nes-Gli3* cko brains as means of samples from three different animals +/− SEM. Student's *t*-test was performed. (M–O) H+E staining

of E10.5 sagittal embryo sections. Note the increased size of the ventricle and increased thickness and abnormal morphology of the Is/r1 region in *Gli3*$^{-/-}$ mutants and *En1-Gli3* cko mutants. (P) Left: Schematic of Shh and Gli expression in the ventral (V) and dorsal (D) embryonic mes/r1. Right: Shh signaling in the ventral and dorsal mes/r1: High levels of Shh induce Gli activator (GliA2/3; green) and inhibit (red) the formation of Gli3 repressor ventrally (Gli3R, purple). Low levels of Shh decrease the formation of Gli3R dorsally. Gradients indicate high to low levels of expression/signaling. Scale bar: (A–H) 500 μm; (I–K, M–N) 250 μm

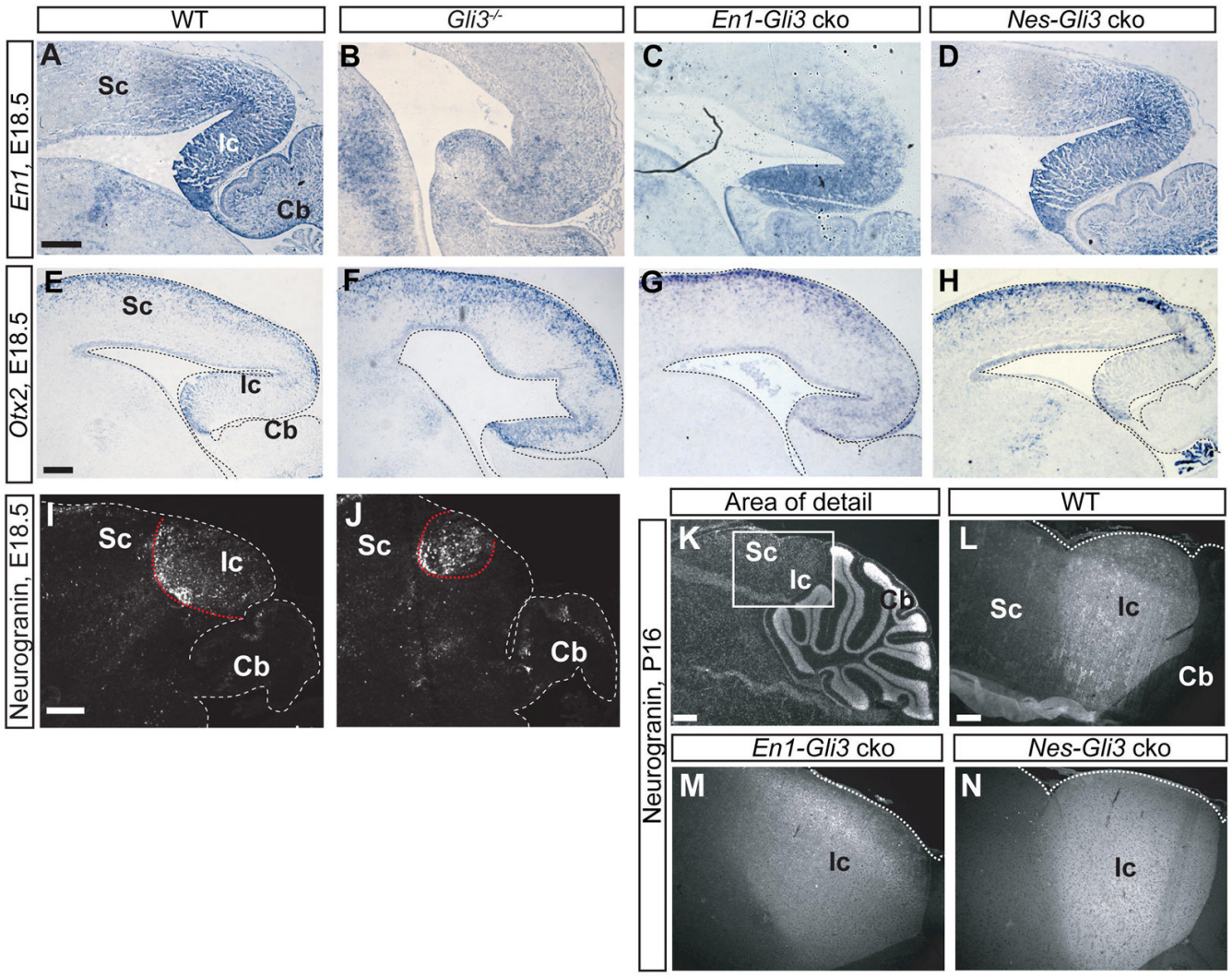

Fig. 2. *Gli3* is required for proper establishment of the inferior colliculus

(A–D) *En1 RNA* expression in the E18.5 inferior colliculus (Ic) and posterior superior colliculus (Sc) in WT sagittal sections (A). *En1* expression is severely reduced in *Gli3*$^{-/-}$ mutants, slightly reduced in *En1-Gli3* cko and normal in *Nes-Gli3* cko mutants (B–D). (E–H) Expression of *Otx2 RNA* in superficial layers of the Sc and the ventricular layer of the Ic is comparable in WT (E) and *Nes-Gli3* cko brains (H). In *Gli3*$^{-/-}$ and *En1-Gli3* cko mutants *Otx2* is expressed throughout the posterior tectum and the thickness of the *Otx2* positive layer is increased in the Sc (F,G). (I,J) Immunohistochemistry for Neurogranin on E18.5 sagittal sections. The Neurogranin positive domain (outlined in red) is reduced and shifted posteriorly in *Gli3*$^{-/-}$ mutants. (K–N) DAPI staining (K) and immunohistochemistry for Neurogranin (L–N) at P16 shows that the Ic is abnormally shaped in *En1-Gli3* cko, but not in *Nes-Gli3* cko mutants. Scale bars: (A–H,I,J,L–N) 250 μm; (K) 500 μm.

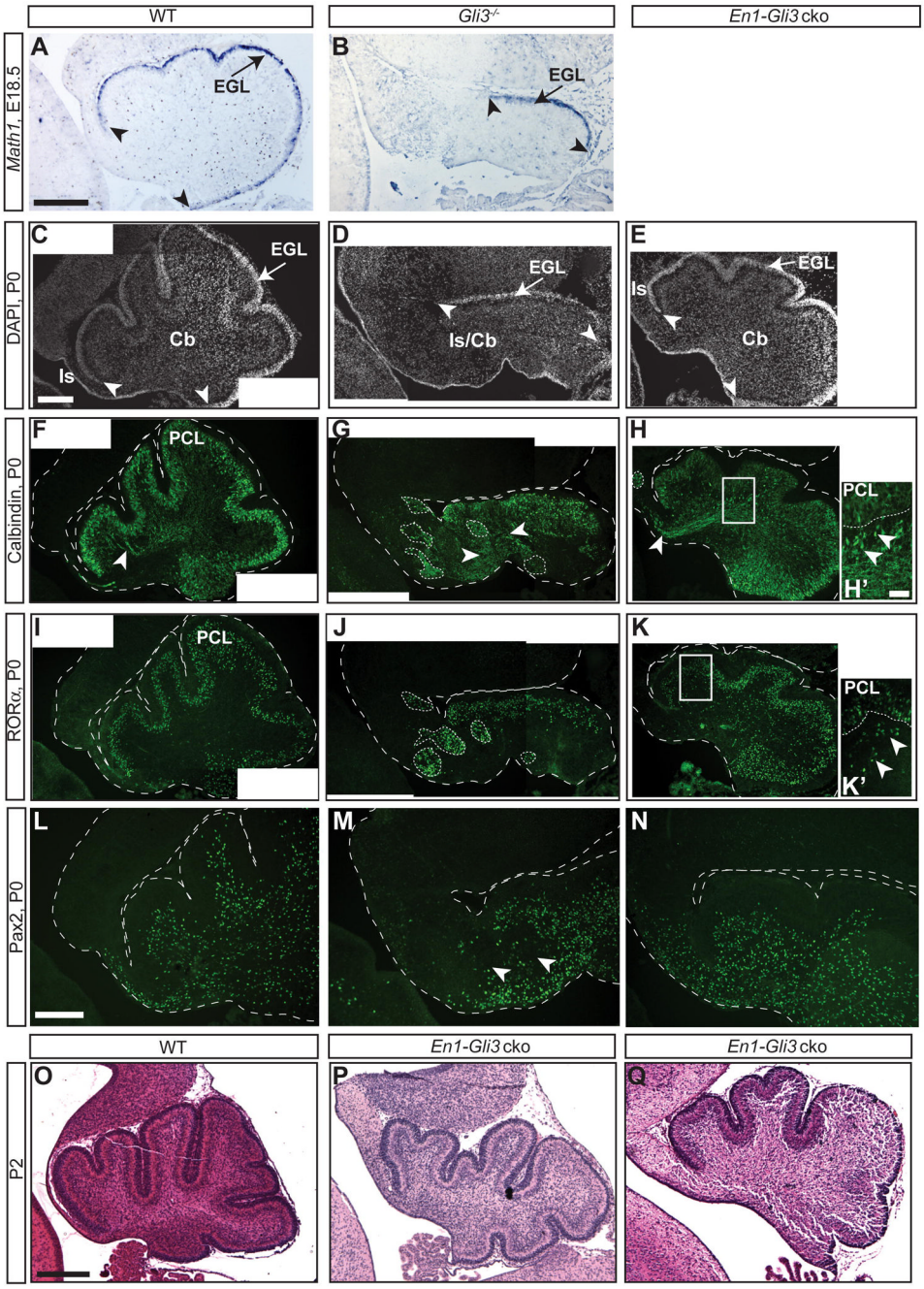

Fig. 3. *Gli3* regulates proper establishment of the isthmus and cerebellum

(A–E) RNA in situ hybridization for *Math1* and DAPI staining shows that the external granule cell layer (EGL) is absent form the most posterior and anterior parts (arrowheads) of the isthmus-cerebellar like (Is/Cb) region in *Gli3*$^{-/-}$ mutants, but is comparable to WT in *En1-Gli3* cko mutants (arrowheads). (F–N) Immunohistochemistry on adjacent sections. (F–K) In the WT, Calbindin and RORα (green) positive Purkinje cells (PC) are organized in a several-cell-deep layer (PCL) underlying the EGL and project into the deeper Cb (arrowheads). In *Gli3*$^{-/-}$ mutants, only a rudimentary PCL forms with disorganized projections (arrowheads), and many PC remain in clusters in the deeper Is/Cb (outlined). (H,K) In *En1-Gli3* cko mutants, most PC are located within the PCL, with only some scattered PC in the underlying areas (H

′,K′, arrowheads) and in ectopic clusters in the anterior Is (outlined). Some PC axons project into the Is (H, arrowhead). (L–M) Pax2 (green) is expressed in a scattered pattern throughout the Is and Cb (except the EGL and PCL) in WT and *En1-Gli3* cko mutants but is not expressed in the anterior (EGL-free) region in $Gli3^{-/-}$ mutants and is excluded from the PC clusters (M, arrowheads). (O–Q) H+E staining of P2 sagittal sections shows the abnormal foliation pattern in *En1-Gli3* cko mutants. Brain regions are outlined where necessary. Note that some of the presented pictures are composites of two images (C,D,F,G,I,J) Scale bars: (A–N) 200 μm; (H ′, K′) 20 μm; (P–Q) 500 μm

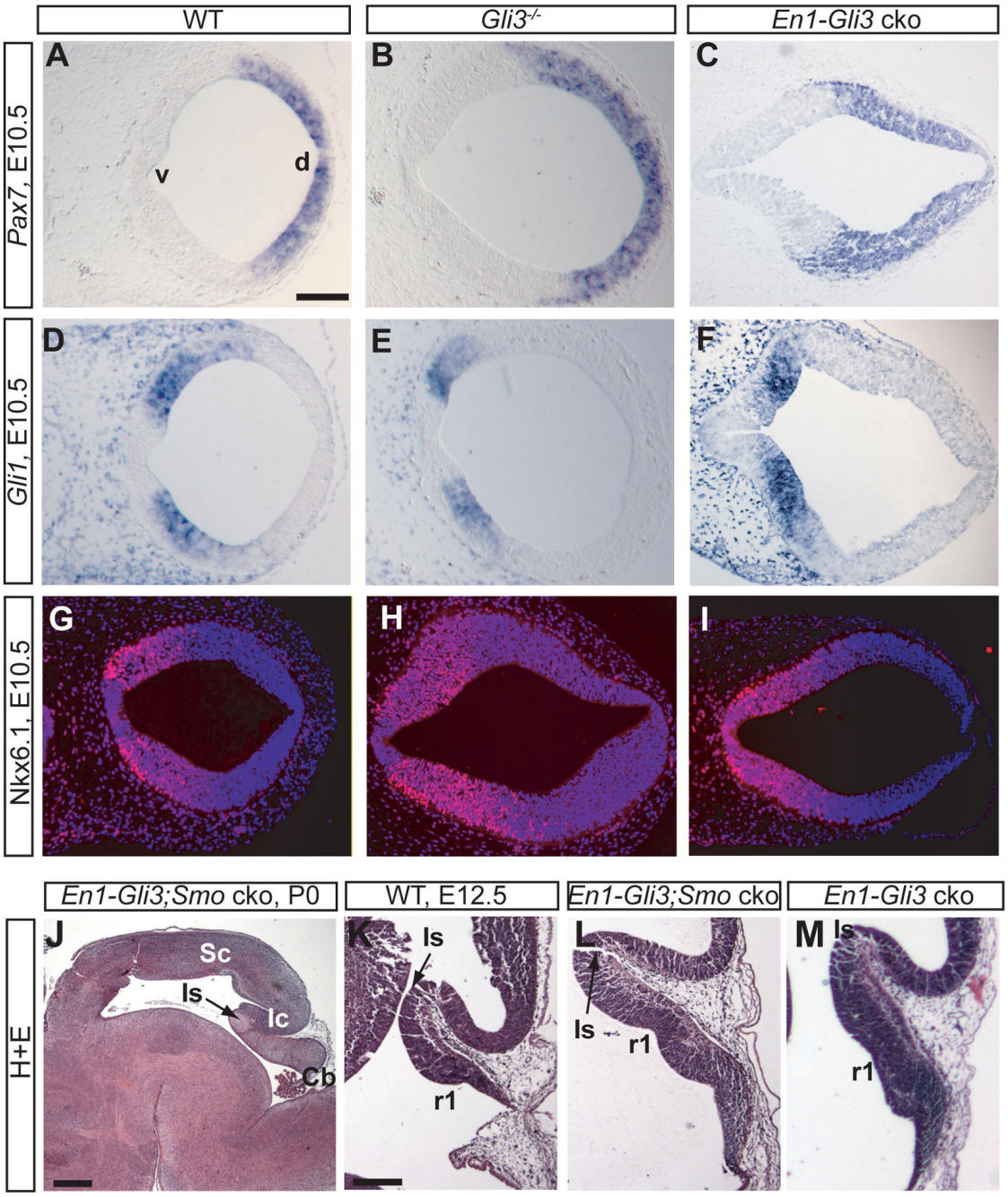

Fig. 4. *Gli3* is not required to establish DV gene expression domains or to inhibit activating Shh signaling

(A–I) *RNA* in situ hybridization for *Pax7* (A–C, dorsal marker) and *Gli1* (D–F, ventral marker) and immunohistochemistry for Nkx6.1 on E10.5 transverse sections (G–I, ventral marker) shows that expression of these genes is comparable to WT in $Gli3^{-/-}$ and *En1-Gli3* cko mutants. (J–M) H+E staining on P0 (J) and E12.5 (K–M) sagittal sections. The phenotype of the Sc, Ic and Is in P0 *En1-Gli3;Smo* cko mutants is comparable to *En1-Gli3* cko mutants. Note that the Cb is small and unfoliated, with a thin external granule cell layer. (K–M) At E12.5, the size of r1 is increased in both *En1-Gli3* and *En1-Gli3;Smo* cko mutants compared to WT. The neural

tube is outlined where necessary. v (ventral), d (dorsal). Scale bars: (A–I) 125 μm, (J) 500 μm, (K–M) 200 μm.

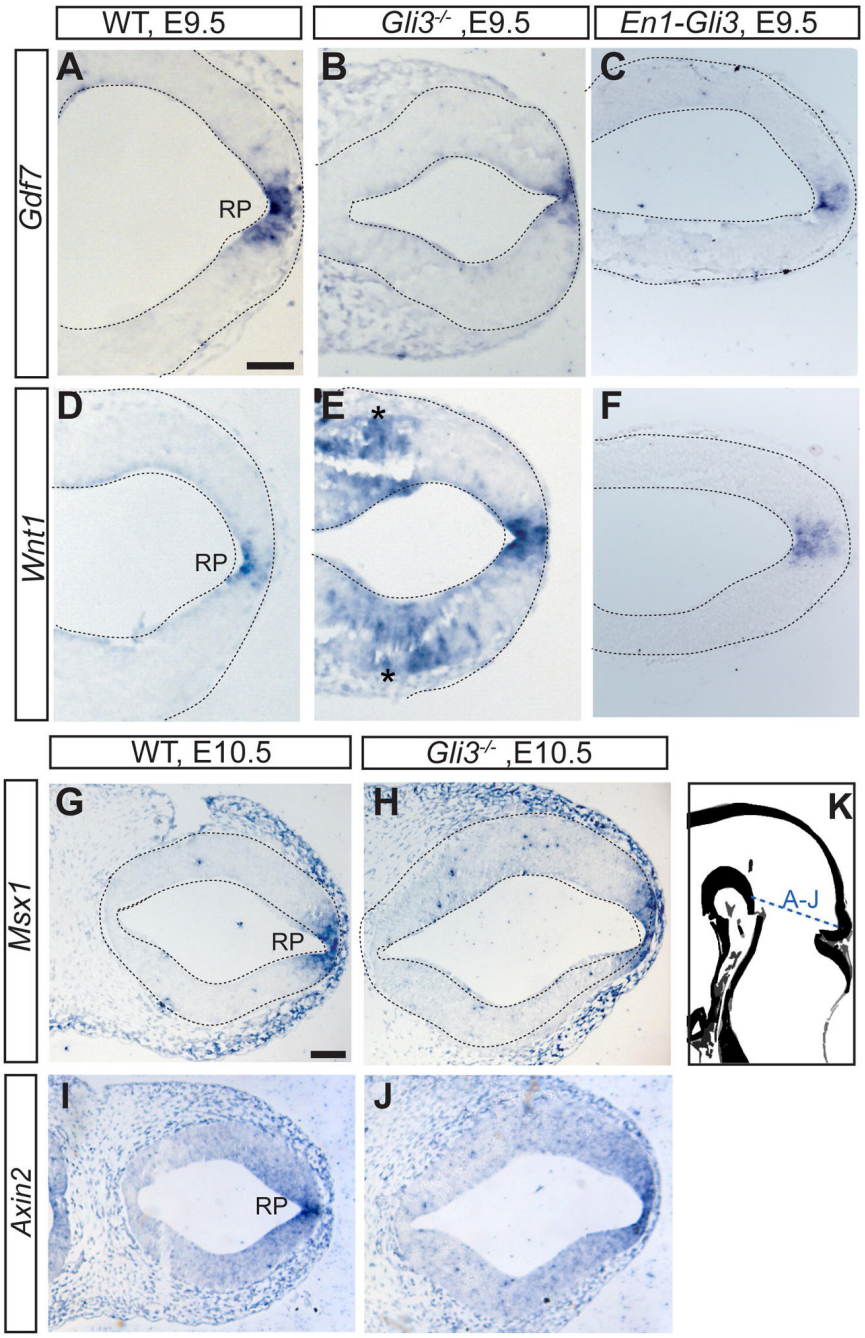

Fig. 5. *Gli3* is not required to establish the mes/r1 roof plate

(A–F) *RNA* in situ hybridization for *Gdf7* and *Wnt1* on E9.5 transverse sections. *Gdf7* and *Wnt1* are expressed in the roof plate (RP) in the WT and mutant embryos. Note that the *Wnt1* positive domain in the lateral mes (*) is in the isthmic region. (G–J) *RNA* in situ hybridization for *Msx1* and *Axin2* on E10.5 transverse sections shows that RP expression is not changed in $Gli3^{-/-}$ mutants. (K) Plane of sections are indicated in the schematic. The neural tube is outlined where necessary. Scale bars: (A–J) 100 μm.

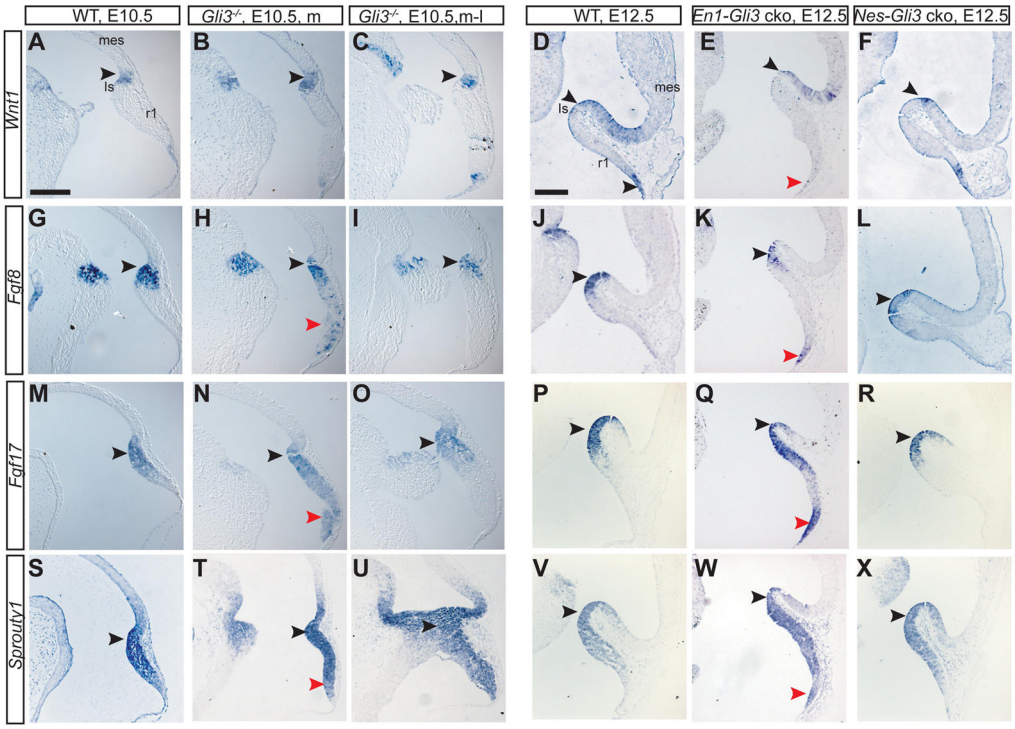

Fig. 6. *Gli3* is required to restrict *Fgf* expression to the isthmus

Fgf8, Fgf17, Spry1 and *Wnt1 RNA* expression. Posterior mes, Is and r1 are shown (see Fig. 5K). Black arrowheads indicate normal, red arrowheads ectopic gene expression. (A–F) The *Wnt1* expression domain is unaltered in *Gli3* mutants. *Fgf8* (G–I), *Fgf17* (M–O), and *Spry1* (SU) domains are expanded into medial, but not lateral r1 in E10.5 $Gli3^{-/-}$ mutants. In E12.5 *En1-Gli3* cko mutants, ectopic expression of *Fgf8* (J,K), *Fgf17* (P,Q), and *Spry1* (V,W) is restricted to the most posterior region of medial r1, where *Wnt1* (D,E) is normally expressed. (L,R,X) *Fgf8, Fgf17,* and *Spry1* gene expression is normal in *Nes-Gli3* cko mutants. Scale bars: 200 μm.

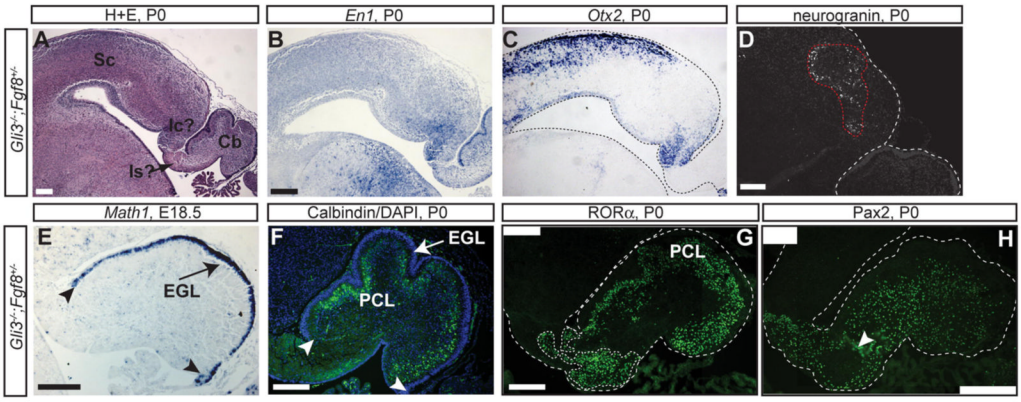

Fig. 7. Partial rescue of *Gli3*$^{-/-}$ mutant phenotype in *Gli3*$^{-/-}$; *Fgf8*$^{+/-}$ mutants

(A) H+E staining on *Gli3*$^{-/-}$;*Fgf8*$^{+/-}$ mutant sagittal sections. The morphology of the Cb and Is, but not of the tectum (Sc and Ic), appears to be partially rescued in *Gli3*$^{-/-}$;*Fgf8*$^{+/-}$ mutants. (C–D) *En1* and *Otx2 RNA* expression and immunohistochemistry for Neurogranin (D, red outline) show that the Ic is not properly established in *Gli3*$^{-/-}$;*Fgf8*$^{+/-}$ mutants. (E,F) *Math1 RNA* expression (E) and DAPI staining (F, blue) show that the EGL expands from the posterior Cb to the Is (arrowheads), comparable to WT. (F,G) Immunohistochemistry for Calbindin and RORα (green) show a relative normal PCL, but a significant number of PCs are located in clusters in the deeper Cb and Is (G, outlined). (H) Pax2 (green) positive cells are found in the Is, but are excluded from PC clusters (arrowhead). Scale bars: 200 μm.

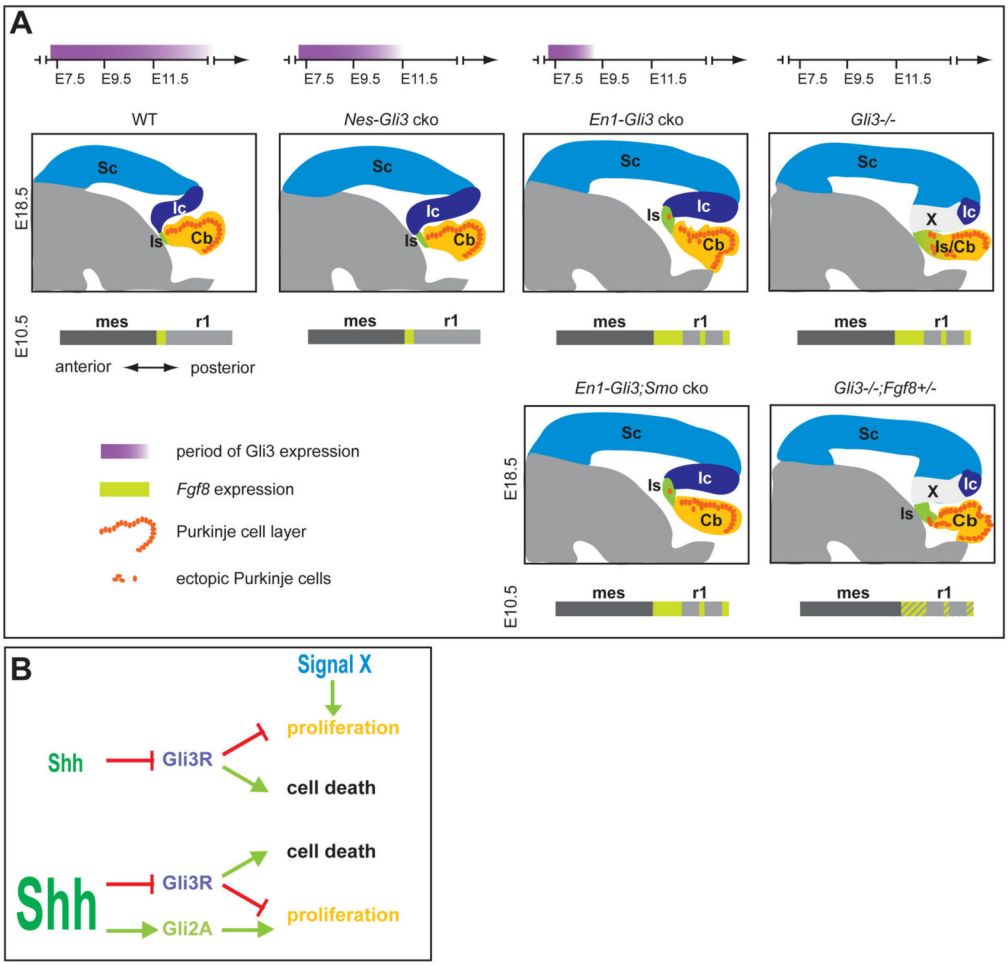

Fig. 8. The distinct temporal roles of Gli3R in regulating mes/r1 development

(A) Time period of *Gli3* gene expression, prenatal tectum and cerebellum phenotype and ectopic *Fgf8* expression. Note that in *Gli3*$^{-/-}$ mutants, a domain (X) forms between the tectum and cerebellum that is not properly specified as cerebellum (Cb), isthmus (Is) or inferior colliculus (Ic). Superior colliculus (Sc). See discussion for details (B) High levels of Shh (lower pathway) regulate mes/r1 growth through induction of proliferation through Gli2A and/or inhibition of cell death through Gli3R. Low levels of Shh (upper pathway) do not induce proliferation, but modulate cell death and proliferation (induced by unknown signal (X)) through the regulation of Gli3R levels.